

Journal of Materials Chemistry C

Accepted Manuscript



This is an *Accepted Manuscript*, which has been through the Royal Society of Chemistry peer review process and has been accepted for publication.

Accepted Manuscripts are published online shortly after acceptance, before technical editing, formatting and proof reading. Using this free service, authors can make their results available to the community, in citable form, before we publish the edited article. We will replace this *Accepted Manuscript* with the edited and formatted *Advance Article* as soon as it is available.

You can find more information about *Accepted Manuscripts* in the [Information for Authors](#).

Please note that technical editing may introduce minor changes to the text and/or graphics, which may alter content. The journal's standard [Terms & Conditions](#) and the [Ethical guidelines](#) still apply. In no event shall the Royal Society of Chemistry be held responsible for any errors or omissions in this *Accepted Manuscript* or any consequences arising from the use of any information it contains.

Tunable cooperativity in a spin-crossover Hoffman-like metal-organic framework material by Aromatic Guests

Cite this: DOI: 10.1039/x0xx00000x

Received 00th January 2012,
Accepted 00th January 2012

DOI: 10.1039/x0xx00000x

www.rsc.org/

Jin-Yan Li, Chun-Ting He, Yan-Cong Chen, Ze-Min Zhang, Wei Liu, Zhao-Ping Ni* and Ming-Liang Tong*

A spin-crossover Hoffman-like metal-organic framework, $[\text{Fe}(\text{dpb})\{\text{Au}(\text{CN})_2\}_2] \cdot n\text{Solv}$ (dpb = 1,4-di(pyridin-4-yl)benzene; $n\text{Solv} = 1.5\text{DMF} \cdot 0.3\text{EtOH} \cdot 0.2\text{C}_6\text{H}_{12}$), is prepared and presents appreciable porosity. By introducing different aromatic guest molecules (benzene, naphthalene, anthracene, ferrocene) and carbon disulfide into this framework, the spin-crossover cooperativity is dramatically modulated. The thermal hysteresis width is tuned from 0 K to 73 K by replacing the original solvents with naphthalene in the 1D channel. DFT calculations are carried out to evaluate the optimized positions of guests and offer an insight into the relationship between spin-crossover cooperativity and host-guest interaction. As a result, significant $\pi \cdots \pi$ stacking interactions (or $\text{S} \cdots \text{Au}$ contact) between host framework and aromatic guest molecules (or CS_2) are responsible for the strong cooperativity.

Introduction

It is feasible that the derivatives of d^4 - d^7 metal ions can adopt high spin state or low spin state electronic configurations.¹ The change between two spin states under external perturbations (temperature, pressure, light, magnetic field, etc.) is referred to as spin crossover (SCO).² It is usually accompanied by the remarkable change of colour, magnetism, dielectric constant, optical properties, and so on.³ Hence, such materials are promising for the development of advanced nanodevices, including displays, storages, sensors and switches.⁴ The occurrence of SCO behavior is fundamentally rationalized on ligand-field theory. However, to achieve a technologically useful SCO material, a most challenging part is controlling the spin transition type (hysteresis, abruptness, etc.), which is determined by the SCO cooperativity. It propagates the spin-transition throughout the bulk materials and can be described by the theory of elastic interaction.⁵

To improve the SCO cooperativity in the solid lattice, a common and effective approach is introducing the intermolecular interactions between the individual SCO metal centers, especially through $\pi \cdots \pi$ stacking or hydrogen bonding.⁶ Secondly, the SCO centers can be bridged by the covalent bonding to form polynuclear compounds or polymer species to enhance cooperativity.^{2c,7} Furthermore, adjusting the host-guest interaction in SCO metal-organic frameworks (MOF)

will combine the benefits of above two strategies and provide multipath communication of elastic interaction. For example, 3 K and 10 K thermal hysteresis were observed when methanol and ethanol guests were introduced into the nanoporous MOF $[\text{Fe}(\text{bpbd})_2(\text{NCS})_2]$ (bpbd = 2,3-bis(4'-pyridyl)-2,3-butanediol), respectively.⁸ The width of hysteresis for $[\text{Fe}(\text{pz})\{\text{Pt}(\text{CN})_4\}]$ (pz = pyrazine) was modulated from 24 K to 64 K with the inclusion of thiourea guest in its pore.⁹ In this respect, nanoporous SCO framework provides a fascinating platform to obtain differing degrees of cooperativity by controlling the host-guest interaction.¹⁰ Scientists have already made a certain extent of progress in guest-effected porous SCO systems in recent decades.¹¹ However, further breakthroughs still need to be made to construct guest-effected SCO framework with strong cooperativity. To gain this goal, rational designs of stable microporous frameworks with well-modulating SCO properties and selections of suitable guests exhibiting strong host-guest interactions are exceptionally significant challenges.

In our group, we reported two guest-effected SCO frameworks, $[\text{Fe}(\text{dpb})\{\text{Ag}(\text{CN})_2\}\{\text{Ag}_2(\text{CN})_3\}] \cdot n\text{Solv}$ (1,4-di(pyridin-4-yl)benzene = dpb)¹² and $[\text{Fe}(2,5\text{-bpp})\{\text{Au}(\text{CN})_2\}_2] \cdot n\text{Solv}$ (2,5-bis(pyrid-4-yl)pyridine = 2,5-bpp)¹³. In the latter case, we used the hydrogen bonding strategy (H-accepting porous coordination polymer and H-donating guests) to construct strong host-guest interactions. An asymmetric two-step SCO behaviour with 23 and 18 K

hysteresis loops can be obtained by introducing *sec*-butanol into the porosity. To further pursue strong SCO cooperativity, here we choose the $\pi \cdots \pi$ stacking strategy. A series of aromatic guests are introduced into a new SCO framework [Fe(dpb){Au(CN)₂}₂] (**1**). Amazingly, a 73 K of thermal hysteresis loop is presented when the naphthalene guest is introduced.

Results and discussion

Synthesis

The crystals of as-synthesized complex, [Fe(dpb){Au(CN)₂}₂] \cdot 1.5DMF \cdot 0.3EtOH \cdot 0.2C₆H₁₂, were obtained by diffusion technique. The organic ligand dpb (0.05 mmol, 12 mg) and K[Au(CN)₂] (0.10 mmol, 29 mg) were dissolved in DMF while Fe(ClO₄)₂ \cdot 9H₂O in EtOH. Then a mixture of DMF, EtOH and C₆H₁₂ acted as the buffer solution. Yellow plate crystals were collected after three weeks. Yield: 70%. The disordered solvent molecules were determined by elemental analysis and TG-MS analysis. Elemental analysis calcd (%) for C_{26.3}H_{26.7}N_{7.5}O_{1.8}Au₂Fe: C 34.10, H 2.90, N 11.34; found: C 33.90, H 2.77, N 11.60. IR data (KBr, cm⁻¹): ν = 3448 (m), 3056 (m), 2923 (m), 2844 (m), 2454 (w), 2173 (s), 1677 (s), 1610 (s), 1552 (m), 1484 (s), 1386 (s), 1216 (m), 1087 (s), 1012 (m), 811 (s), 719 (s).

1 \cdot (1.5)C₆H₁₂ was obtained by the immersion of as-synthesized complex in pure cyclohexane solvent for two weeks (solvent is refreshed every day). The completeness of solvent exchange and amount of solvent molecule were determined by TG-MS analysis. **1** \cdot (1.5)C₆H₁₂ was heated on thermogravimetric analyser (N₂ atmosphere) at 100 °C for three hours to form the desolvated sample **1**. Elemental analysis calcd (%) for **1** \cdot (1.5)C₆H₁₂ (C₂₉H₃₀N₆Au₂Fe): C 38.18, H 3.31, N 9.21; found: C 38.15, H 3.24, N 9.19. Desolvated sample **1** (C₂₀H₁₂N₆Au₂Fe): C 30.56, H 1.54, N 10.69; found: C 30.77, H 1.71, N 10.45.

Guest adsorption: The guest adsorption procedures were performed by inserting a tube with desolvated samples into vessels with different guest molecules at room temperature for two days for **1** \cdot (0.9)Benzene, **1** \cdot (1.4)CS₂ and **1** \cdot (0.7)Naphthalene, while at 75 °C and 100 °C for 6 hours for **1** \cdot (0.4)Ferrocene and **1** \cdot (0.3)Anthracene, respectively. Elemental analysis calcd (%) for **1** \cdot (0.4)Ferrocene (C₂₄H₁₆N₆Au₂Fe_{1.4}): C 33.50, H 1.87, N 9.77; found: C 33.86, H 1.86, N 9.88.

Structure

Single crystal X-ray diffraction data of as-synthesized complex were collected at 95 K and 250 K. It adopts the monoclinic space group *P2(1)/m* at both measured temperatures. All the iron centers are crystallographically equivalent and in a distorted [FeN₆] octahedral coordination environment. As displayed in Figure 1, the octahedral Fe^{II} centers are linked equatorially by four separate linear [Au(CN)₂]⁻ species, generating [Fe{Au(CN)₂}₂]_∞ 2D layers with [Fe₄{Au(CN)₂}₄] grids of dimension 10.47 Å \times 10.44 Å. Meanwhile, the axial

sites are occupied by nitrogen atoms from dpb ligands which pillar the layers, leading to 3D network (Figure 2). Moreover, two identical networks are interpenetrated to each other, resulting in a 3D interpenetrated framework in which two closest [Fe{Au(CN)₂}₂]_∞ layers exist obvious aurophilic interactions (Au \cdots Au: 3.11 Å at 95 K, 3.14 Å at 250 K), see Figure S1 and S2. Despite the interpenetration, this framework displays 1D channel along *b* axis where the disordered solvent molecules are housed. After moving away the disordered solvent molecules by SQUEEZE,¹⁴ the appreciable void space is 787.5 Å³ per unit cell (46.9 % of the volume) at 250 K. The phenyl ring of dpb is perpendicular to channel while one pyridyl ring is disordered, which blocks the aperture to some extent, leading to a corrugated channel with size of 9.6 Å \times 4.1 Å, see Figure S3. Upon cooling, the crystals exhibited a remarkable colour change from yellow to red (Figure S4), implying a spin-transition of iron sites. The average Fe-N distances are 1.95 Å at 95 K and 2.17 Å at 250 K, varying by approximately 0.22 Å. On the other hand, the change of the unit-cell volume is 133.11 Å³, representing 8% of the volume in HS state. The above two characteristic structural changes corroborate the spin-transition of iron(II).¹⁵

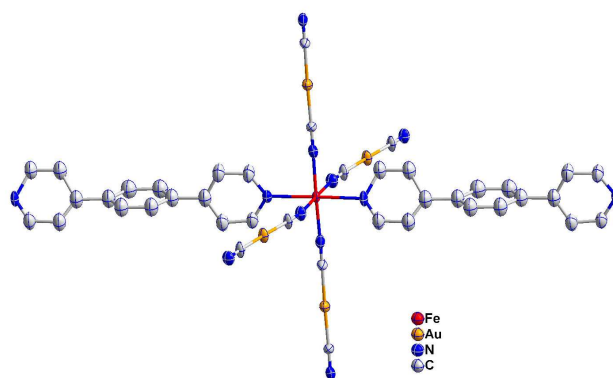


Figure 1. A fragment of as-synthesized complex showing coordination environment. The thermal ellipsoids are drawn at the 50% probability. And all hydrogen atoms are omitted for clarity.

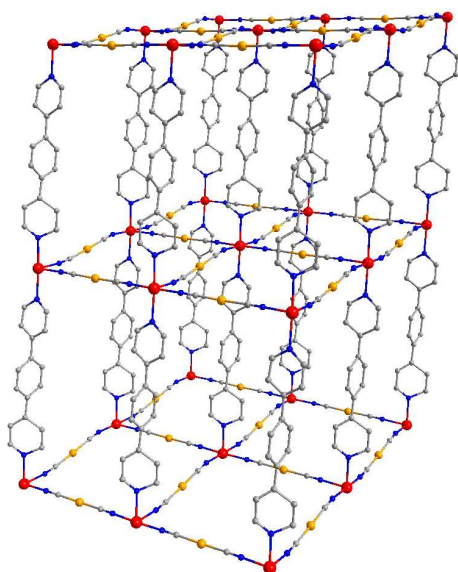


Figure 2. View of one 3D network in as-synthesized complex. All hydrogen atoms are omitted for clarity. Fe: red, Au: yellow, N: blue, C: grey.

Magnetic properties

The magnetic susceptibility measurements were carried out and their plots are depicted in Figure 3. For the as-synthesized complex, it undergoes a gradual and complete one step spin-transition. The $\chi_M T$ value is nearly constant at $3.50 \text{ cm}^3 \text{ K mol}^{-1}$ until 240 K, implying one iron(II) of HS state. Lowering the temperature further, it decreases to a minimum value of $0.19 \text{ cm}^3 \text{ K mol}^{-1}$ at 100 K, with the critical temperature of 175 K. This indicates that all the iron(II) centers take place the changes from HS to LS states. To obtain the intact desolvated framework, we performed cyclohexane solvent exchange with the as-synthesized complex before its desolvation. In the case of $\mathbf{1} \cdot (1.5)\text{C}_6\text{H}_{12}$, a gradual and incomplete spin-transition involving 60% of iron centers is presented. Its critical temperatures are 136 K and 142 K in the cooling and warming modes, respectively, defining a 6 K thermal hysteresis loop. The desolvated sample **1** displays an incomplete (77% of iron(II) centers involved) and unsymmetric two-step SCO behavior with 9 K thermal hysteresis loop for the low-temperature step ($T_{c1} = 156 \text{ K}$; $T_{c2\downarrow} = 119 \text{ K}$, $T_{c2\uparrow} = 110 \text{ K}$).

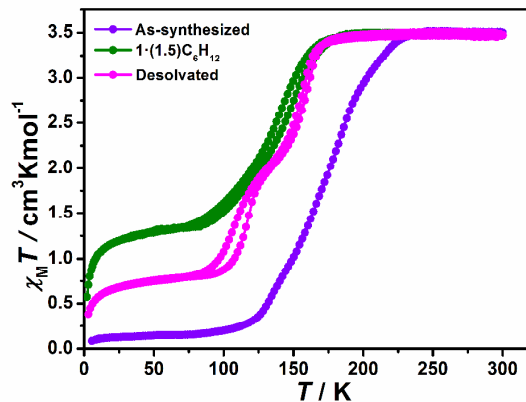


Figure 3. Plots of $\chi_M T$ vs. T for as-synthesized complex, $\mathbf{1} \cdot (1.5)\text{C}_6\text{H}_{12}$ and desolvated analogue.

In view of the characteristics of this framework, the variable-temperature magnetic measurements for the clathrates of CS_2 and aromatic guests are performed to get an improvement of SCO cooperativity (Figure 4). Concerning the smallest guest carbon disulfide, the $\mathbf{1} \cdot (1.4)\text{CS}_2$ undergoes abrupt one-step SCO behavior together with 23 K width thermal hysteresis. Its critical temperatures are 167 K and 190 K for the cooling and warming processes, respectively.

For the aromatic guests, 83% of iron(II) centers take place the spin state change in $\mathbf{1} \cdot (0.9)\text{Benzene}$, which reveals asymmetric three steps SCO property. The critical temperatures are $T_{c1\downarrow} = 207 \text{ K}$, $T_{c1\uparrow} = 221 \text{ K}$, $T_{c2} = 155 \text{ K}$, $T_{c3\downarrow} = 139 \text{ K}$ and $T_{c3\uparrow} = 144 \text{ K}$, that is, there are 14 K and 5 K thermal hysteresis loops for the first and third steps, respectively. When the guest replaced by naphthalene, the $\mathbf{1} \cdot (0.7)\text{Naphthalene}$ shows a relatively cooperative spin-transition involving 75% of iron(II) centers. It undergo an abrupt one-step SCO behavior with $T_{c\downarrow} = 141 \text{ K}$ in the cooling process. However, it shows gradual two-step spin transition without obvious plateau in the sequential warming mode. The critical temperature of $T_{c\uparrow}$ is generally considered to be 214 K, if we regard it as one-step SCO tentatively. Then they define a 73 K width hysteresis loop for $\mathbf{1} \cdot (0.7)\text{Naphthalene}$. As for $\mathbf{1} \cdot (0.3)\text{Anthracene}$ and $\mathbf{1} \cdot (0.4)\text{Ferrocene}$, they show gradual incomplete spin transition in the cooling process, while complicated steps in the warming process. The widths of hysteresis loops are supposed to be 20 K ($T_{c\downarrow} = 131 \text{ K}$, $T_{c\uparrow} = 151 \text{ K}$) and 37 K ($T_{c\downarrow} = 129 \text{ K}$, $T_{c\uparrow} = 166 \text{ K}$) for $\mathbf{1} \cdot (0.3)\text{Anthracene}$ and $\mathbf{1} \cdot (0.4)\text{Ferrocene}$, respectively.

Such stepwise SCO behaviours mentioned above are not unusual. We tentatively ascribe these phenomena to the disorder of guests and dpb ligand¹⁶ or symmetry breaking phase transition¹⁷ as other examples. Unfortunately, they are hardly detected by standard measuring instruments for the present cases.

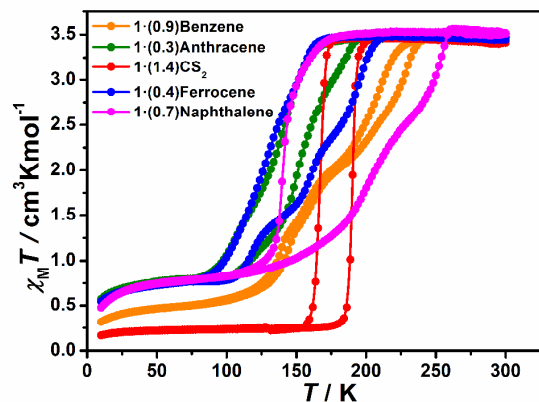


Figure 4. Temperature dependence of $\chi_M T$ curves for different clathrates.

DFT calculation

The magnetic measurements show that the hysteresis widths are dramatically tunable. It is well worth further investigating the magno-structural relationship. As evidenced by the powder X-ray diffraction (Figure S5), all samples present similar frameworks whatever guests introduced into the pore. Hence,

the variations of SCO properties for different clathrate complexes mainly result from the natures of guests and host-guest interactions.

In order to give a deep insight into the host-guest interactions, we carried out Density Functional Theory (DFT) calculation for these clathrates (see computational details in supporting information). According to the optimized results of DFT calculation, all the clathrates exhibit significant intermolecular interactions between guest molecules and the host framework as shown in Table 1 and Figure 5. As expected, the calculation results show that the edge-to-face C-H \cdots π interactions or offset $\pi\cdots\pi$ interactions are observed between the framework and aromatic guest molecules. Meanwhile, S \cdots Au^I contact is noted in 1·(1.4)CS₂. Thus, in addition to the communication of cooperativity by covalent bonding in the framework, the host-guest interaction provides a new path to transmit the cooperativity in the lattice. These intermolecular interactions would be treated as “chemical pressure”¹⁸ and influence the efficiency of transmitting cooperativity in the lattice.^{1b,2c,19}

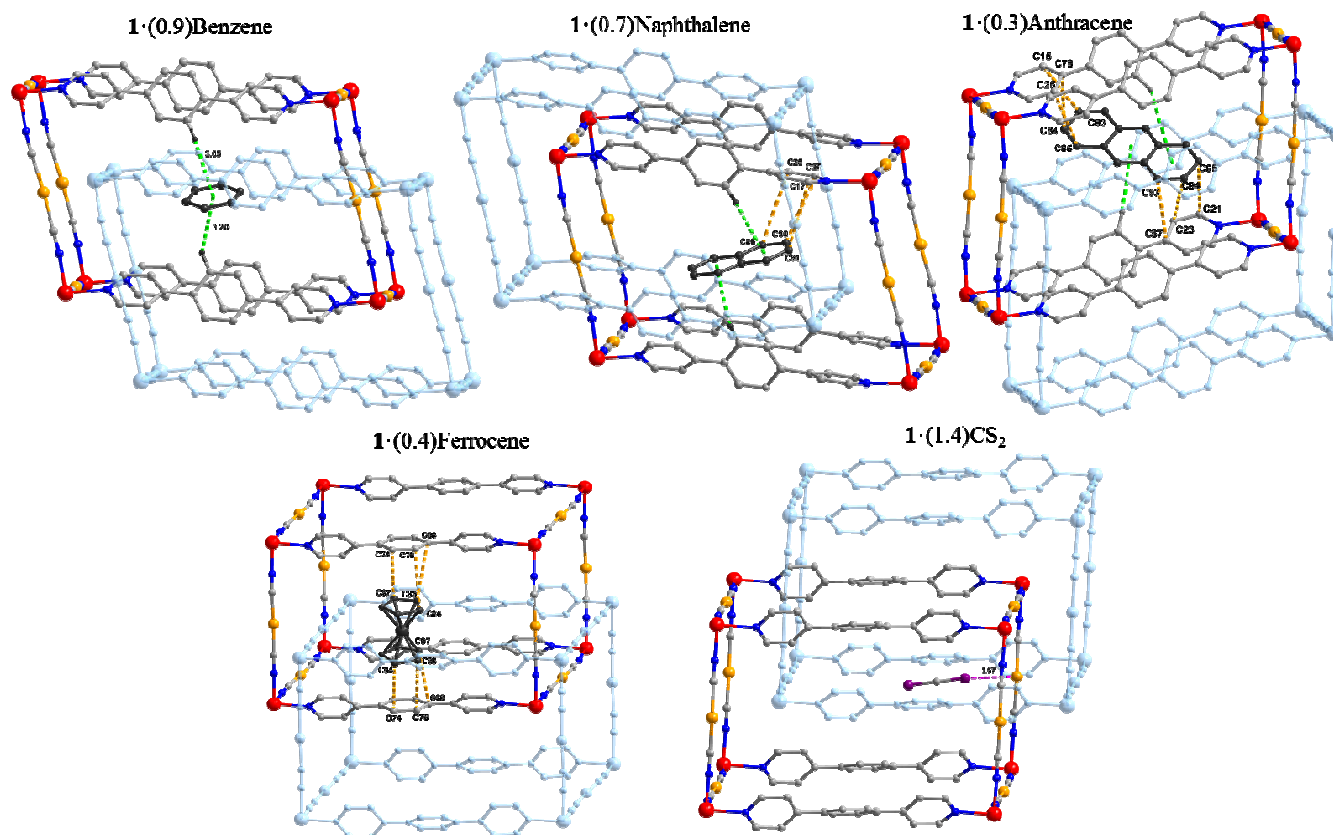


Figure 5. Optimized positions of guests and host-guest interactions. Dot lines: green, C-H \cdots π distance; yellow, C \cdots C distance; magenta, Au \cdots S distance.

ARTICLE

Table 1. Selected distances [\AA] and thermal hysteresis width [K] for different clathrates.

| clathrate | C-H $\cdots\pi$ | offset $\pi\cdots\pi$ | S \cdots M ^I | ΔT |
|--------------------------------|-----------------|-------------------------|---------------------------|------------|
| 1 ·(0.9)Benzene | 3.05/3.20 | – | – | 5/14 |
| 1 ·(0.7)Naphthalene | 2.95/3.12 | 3.69–4.05 | – | 73 |
| 1 ·(0.3)Anthracene | 3.51/4.00 | 3.86–4.14, 3.60–3.79 | – | 20 |
| 1 ·(0.4)Ferrocene | – | 3.60–3.77, 3.52–3.72 | – | 37 |
| 1 ·(1.4)CS ₂ | – | – | 3.57 | 23 |

Firstly, we focus on the guests of hexatomic-aromatic derivatives. When the benzene introduced into pores of the framework, **1**·(0.9)Benzene displays wider thermal hysteresis loop than the desolvated analogue. This would be attributed to the significant edge-to-face C-H $\cdots\pi$ interaction between the framework and benzene guest, which can improve the lattice cooperativity. Such contact is defined by the distance of the H in phenyl ring of dpb ligand to the centroid of benzene. In the case of **1**·(0.3)Anthracene, it exhibits not only the edge-to-face C-H $\cdots\pi$ interactions between the phenyl ring of dpb and anthracene, but also two offset $\pi\cdots\pi$ interactions involving the pyridyl groups of dpb and guest molecule. These offset $\pi\cdots\pi$ interactions are evaluated by the C \cdots C distance between two related aromatic rings. As a result, the hysteresis width of **1**·(0.3)Anthracene is larger than that of **1**·(0.9)Benzene. With respect to the **1**·(0.7)Naphthalene, it presents the strongest edge-to-face C-H $\cdots\pi$ interactions of 2.95/3.12 \AA . In addition, offset $\pi\cdots\pi$ interaction with the C \cdots C distance of 3.69–4.05 \AA are observed between the naphthalene and pyridyl ring of dpb. These contacts imply relatively strong synergism in **1**·(0.7)Naphthalene, which is certified by its 73 K thermal hysteresis loop.

In terms of the ferrocene, it has been introduced in MOF materials through sublimation process.²⁰ However, only the derivatives of ferrocene have been reported to construct SCO compounds.²¹ To the best of our knowledge, this is the first time that ferrocene plays a role as guest in tuning the SCO behavior. In our work, **1**·(0.4)Ferrocene exhibits 37 K thermal hysteresis width. We made an analysis of its structure and noted two significant offset $\pi\cdots\pi$ interactions between the ferrocene and phenyl ring of dpb. Such interaction would lead to cooperative lattice and be responsible for the hysteresis phenomenon.

In the case of CS₂, it shows a S \cdots Au contact of 3.57 \AA between CS₂ guest and Au^I in the framework. The similar contact has been reported in the {Fe(pz)[Pt(CN)₄]} system,^{9b} in which a S \cdots Pt interaction of 3.405 \AA is observed and the

inclusion of CS₂ results in stabilizing the LS state. In our work, **1**·(1.4)CS₂ undergoes a more complete spin transition with higher critical temperatures than the desolvated sample **1**. Most notably, it displays abrupt SCO behavior with 23 K wide hysteresis, suggesting the strong cooperativity. Reminiscent of {Fe(pz)[Pt(CN)₄]} system, both the crystal orbital displacement (COD) curves of {Fe(pz)[Pt(CN)₄]} with CS(NH₂)₂ and CS₂ suggest that their S \cdots Pt interactions play key roles in the stabilization of the host-guest systems.^{9c,11o} And the strong cooperative spin transition of {Fe(pz)[Pt(CN)₄]}·0.5(CS(NH₂)₂) arises from multiple significant intermolecular interactions.^{9c} Here, the S \cdots Au interaction predicted by the DFT calculation should also be the main part of the host-guest interaction. The situation is that the number of CS₂ is more than one, which may provide the possibility of multiple intermolecular interactions. In addition, it cannot be eliminated that the guest molecule may be disordered, which can also make a contribution to the SCO cooperativity.

Conclusions

In summary, a novel SCO Hoffman-like coordination polymer with appreciable porosity has been reported hereby, which promises to be an appropriate system to modulate the SCO cooperativity by different guests inside. Hence, CS₂ and a series of aromatic guests are introduced into its framework to perform suitable host-guest interactions for enhancement of SCO cooperativity. The widths of thermal hysteresis loop are dramatically changed in these clathrates. Amazingly, the largest hysteresis width can reach 73 K in **1**·(0.7)Naphthalene. And we first adopted ferrocene as guest to modulate spin-transition and obtain a relatively cooperative SCO clathrate. To investigate the relationship between host-guest interaction and SCO property, DFT calculations are carried out to estimate the optimized positions of guests. Significant edge-to-face C-H $\cdots\pi$ interactions or offset $\pi\cdots\pi$ interactions are observed between host and aromatic guests. And S \cdots Au interaction of 3.57 \AA is presented in **1**·(1.4)CS₂. Thus, these intermolecular interactions can be regarded as “chemical pressure” to some extent and may enhance the cooperativity, which are responsible for the different thermal hysteresis phenomena in various clathrates. All in all, porous SCO coordination polymers are fascinating subjects to manipulate magnetic properties through introducing various guests. They also provide a pivotal platform of searching the relation between intermolecular interaction and SCO behaviour. Therefore, although researchers have made a great many achievements in this respect, a greater breakthrough is still worth to be made to achieve a technologically useful SCO material.

Acknowledgements

This work was supported by the “973 Project” (2012CB821704 and 2014CB845602), the NSFC (Grant nos 91122032, 21201182, 21373279 and 91422302) and Program for Changjiang Scholars and Innovative Research Team in University of China.

Notes and references

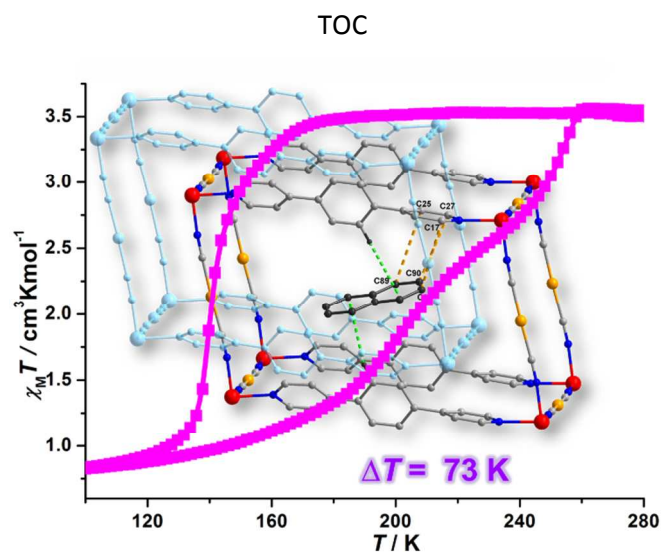
Key Laboratory of Bioinorganic and Synthetic Chemistry of Ministry of Education, School of Chemistry and Chemical Engineering, Sun Yat-Sen University, Guangzhou 510275, P. R. China.

E-mail: tongml@mail.sysu.edu.cn

nizhp@mail.sysu.edu.cn

†Electronic Supplementary Information (ESI) available: Experimental section; crystallographic data of **1**; additional structural pictures; PXRD patterns; crystal photos of **1**; additional magnetic data; TG-MS spectra and TG spectra. CCDC reference numbers 1042076 (**1**_95 K), 1042071 (**1**_250 K). See DOI: 10.1039/b000000x/

- a) P. Gütllich and H. A. Goodwin, *Top. Curr. Chem.*, 2004, **233**, 1; b) M. A. Halcrow, *Coord. Chem. Rev.*, 2009, **253**, 2493; c) G. A. Craig, O. Roubeau and G. Aromí, *Coord. Chem. Rev.*, 2014, **269**, 13.
- a) P. Gütllich, A. Huaser and H. Spiering, *Angew. Chem. Int. Ed. Engl.*, 1994, **33**, 2024; b) O. Kahn and C. J. Martínez, *Science*, 1998, **279**, 44; c) P. Gütllich, Y. Garcia and H. A. Goodwin, *Chem. Soc. Rev.*, 2000, **29**, 419; d) O. Sato, J. Tao and Y.-Z. Zhang, *Angew. Chem. Int. Ed.*, 2007, **46**, 2152.
- J. Tao, R.-J. Wei, R.-B. Huang and L.-S. Zheng, *Chem. Soc. Rev.*, 2012, **41**, 703.
- a) O. Kahn, J. Kröber and C. Jay, *Adv. Mater.*, 1992, **4**, 718; b) W. Fujita and K. Awaga, *Science*, 1999, **286**, 261; c) X. Bao, P.-H. Guo, W. Liu, J. Tucek, W.-X. Zhang, J.-D. Leng, X.-M. Chen, I. Guraslkyi, L.; Salmon, A. Bousseksou and M.-L. Tong, *Chem. Sci.*, 2012, **3**, 1629.
- H. Spiering, *Top. Curr. Chem.*, 2004, **235**, 171.
- M. A. Halcrow, *Spin-Crossover Materials: Properties and Applications*, John Wiley & Sons, Ltd. 2013, 147.
- O. Kahn, E. Codjovi, Y. Garcia, P. J. van Koningsbruggen, R. Lapouyadi and L. Sommier, In: M. M. Turnbull, T. Sugimoto and L. K. Thompson (eds) *Molecule Based Magnetic Materials*, ACS Symposium Series 644, 1996, 298.
- S. M. Neville, G. J. Halder, K. W. Chapman, M. B. Duriska, B. Moubaraki, K. S. Murray and C. J. Kepert, *J. Am. Chem. Soc.*, 2009, **131**, 12106.
- a) S. Bonhommeau, G. Molnár, A. Galet, A. Zwick, J. A. Real, J. J. McGarvey and A. Bousseksou, *Angew. Chem. Int. Ed.*, 2005, **44**, 4069; b) M. Ohba, K. Yoneda, G. Agustí, M. C. Muñoz, A. B. Gaspar, J. A. Real, M. Yamasaki, H. Ando, Y. Nakao, S. Sakaki and S. Kitagawa, *Angew. Chem. Int. Ed.*, 2009, **48**, 4767; c) F. J. Muñoz-Lara, A. B. Gaspar, D. Aravena, E. Ruiz, M. C. Muñoz, M. Ohba, R. Ohtani, S. Kitagawa and J. A. Real, *Chem. Commun.*, 2012, **48**, 4686.
- K. S. Murray and C. J. Kepert, *Top. Curr. Chem.*, 2004, **233**, 195.
- See for example: a) J. A. Real, E. Andrés, M. C. Muñoz, M. Julve, T. Granier, A. Bousseksou and F. Varret, *Science*, 1995, **268**, 265; b) V. Niel, J. M. Martínez-Agudo, M. C. Muñoz, A. B. Gaspar and J. A. Real, *Inorg. Chem.*, 2001, **40**, 3838; c) G. J. Halder, C. J. Kepert, B. Moubaraki, K. S. Murray and J. D. Cashion, *Science*, 2002, **298**, 1762; d) S. M. Neville, B. Moubaraki, K. S. Murray and C. J. Kepert, *Angew. Chem. Int. Ed.*, 2007, **46**, 2059; e) G. Molnár, S. Cobo, J. A. Real, F. Carcenac, E. Daran, C. Vieu and A. Bousseksou, *Adv. Mater.*, 2007, **19**, 2163; f) S. M. Neville, G. J. Halder, K. W. Chapman, M. B. Duriska, P. D. Southon, J. D. Cashion, J.-F. Létard, B. Moubaraki, K. S. Murray and C. J. Kepert, *J. Am. Chem. Soc.*, 2008, **130**, 2869; g) G. J. Halder, K. W. Chapman, S. M. Neville, B. Moubaraki, K. S. Murray, J.-F. Létard and C. J. Kepert, *J. Am. Chem. Soc.*, 2008, **130**, 17552; h) P. D. Southon, L. Liu, E. A. Fellows, D. J. Price, G. J. Halder, K. W. Chapman, B. Moubaraki, K. S. Murray, J.-F. Létard and C. J. Kepert, *J. Am. Chem. Soc.*, 2009, **131**, 10998; i) M. C. Muñoz and J. A. Real, *Coord. Chem. Rev.*, 2011, **255**, 2068; j) R. Ohtani, K. Yoneda, S. Furukawa, N. Horike, S. Kitagawa, A. B. Gaspar, M. C. Muñoz, J. A. Real and M. Ohba, *J. Am. Chem. Soc.*, 2011, **133**, 8600; k) N. F. Sciortino, K. R. Scherl-Gruenwald, G. Chastanet, G. J. Halder, K. W. Chapman, J.-F. Létard and C. J. Kepert, *Angew. Chem. Int. Ed.*, 2012, **51**, 10154; l) F. J. Muñoz-Lara, A. B. Gaspar, M. C. Muñoz, M. Arai, S. Kitagawa, M. Ohba and J. A. Real, *Chem. Eur. J.*, 2012, **18**, 8013; m) X. Bao, H. J. Shepherd, L. Salmon, G. Molnár, M.-L. Tong and A. Bousseksou, *Angew. Chem. Int. Ed.*, 2013, **52**, 1198; n) F. Shao, J. Li, J.-P. Tong, J. Zhang, M.-G. Chen, Z. Zheng, R.-B. Huang, L.-S. Zheng and J. Tao, *Chem. Commun.*, 2013, **49**, 10730. o) D. Aravena, Z. Arcis Castillo, M. C. Muñoz, A. B. Gaspar, K. Yoneda, R. Ohtani, A. Mishima, S. Kitagawa, M. Ohba, J. A. Real and E. Ruiz, *Chem. Eur. J.*, 2014, **20**, 12864.
- J.-Y. Li, Z. Yan, Z.-P. Ni, Z.-M. Zhang, Y.-C. Chen, W. Liu and M.-L. Tong, *Inorg. Chem.*, 2014, **53**, 4039.
- J.-Y. Li, Y.-C. Chen, Z.-M. Zhang, W. Liu, Z.-P. Ni and M.-L. Tong, *Chem. Eur. J.*, 2015, **21**, 1645.
- P. Van Der Sluis and A. L. Spek, *Acta Crystallogr. Sect. A*, 1990, **46**, 194.
- H. J. Shepherd, I. A. Gural'skiy, C. M. Quintero, S. Tricard, L. Salmon, G. Molnár and A. Bousseksou, *Nat. Commun.*, 2013, **4**, 2607.
- a) K. W. Törnroos, M. Hostettler, D. Chernyshov, B. Vangdal and H.-B. Bürgi, *Chem. Eur. J.*, 2006, **12**, 6207; b) D. Chernyshov, N. Klinduhov, K. W. Törnroos, M. Hostettler, B. Vangdal and H.-B. Bürgi, *Phys. Rev. B*, 2007, **76**, 014406/1; c) D. Chernyshov, B. Vangdal, K. W. Törnroos and H.-B. Bürgi, *New J. Chem.*, 2009, **33**, 1277; d) C. Lochenie, W. Bauer, A. P. Railliet, S. Schlamp, Y. Garcia and B. Weber, *Inorg. Chem.*, 2014, **53**, 11563.
- D. Chernyshov, M. Hostettler, K. W. Törnroos and H.-B. Bürgi, *Angew. Chem. Int. Ed.*, 2003, **42**, 3825.
- J.-B. Lin, W. Xue, B.-Y. Wang, J. Tao, W.-X. Zhang, J.-P. Zhang and X.-M. Chen, *Inorg. Chem.*, 2012, **51**, 9423.
- M. A. Halcrow, *Chem. Soc. Rev.*, 2011, **40**, 4119.
- D. Liu, J.-P. Lang and B. F. Abrahams, *J. Am. Chem. Soc.*, 2011, **133**, 11042.
- a) M. Nihei, L. Han and H. Oshio, *J. Am. Chem. Soc.*, 2007, **129**, 5312; b) H. S. Scott, A. Nafady, J. D. Cashion, A. M. Bond, B. Moubaraki, K. S. Murray and S. M. Neville, *Dalton Trans.*, 2013, **42**, 10326; c) H. S. Scott, C. J. Gartshore, S.-X. Guo, B. Moubaraki, A. M. Bond, S. R. Batten and K. S. Murray, *Dalton Trans.*, 2014, **43**, 15212.



The spin-crossover cooperativity of a Hoffman-like metal-organic framework is dramatically modulated by introducing different aromatic guest molecules (benzene, naphthalene, anthracene, ferrocene) with the thermal hysteresis width ranging from 0 K to 73 K.